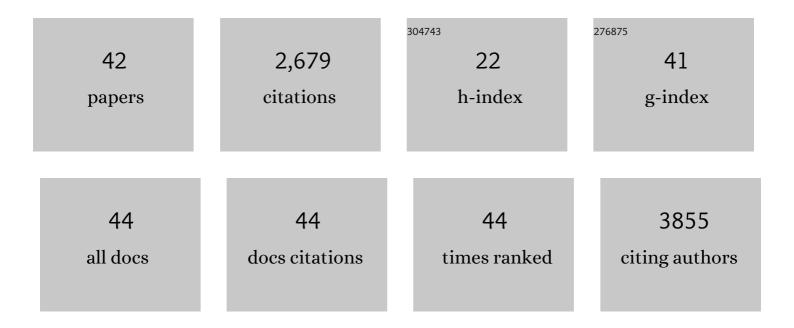
William D Rooney

List of Publications by Year in descending order

Source: https://exaly.com/author-pdf/7476345/publications.pdf Version: 2024-02-01



WILLIAM D ROONEY

#	Article	IF	CITATIONS
1	Metabolic activity diffusion imaging (MADI): II. Noninvasive, highâ€resolution human brain mapping of sodium pump flux and cell metrics. NMR in Biomedicine, 2023, 36, .	2.8	5
2	DCE-MRI of Brain Fluid Barriers: <i>In Vivo</i> Water Cycling at the Human Choroid Plexus. Tissue Barriers, 2022, 10, 1963143.	3.2	6
3	Myelinâ€specific T cells in animals with Japanese macaque encephalomyelitis. Annals of Clinical and Translational Neurology, 2021, 8, 456-470.	3.7	5
4	MRI characteristics of Japanese macaque encephalomyelitis: Comparison to human diseases. Journal of Neuroimaging, 2021, 31, 480-492.	2.0	1
5	The Effect of High Fat Diet on Cerebrovascular Health and Pathology: A Species Comparative Review. Molecules, 2021, 26, 3406.	3.8	18
6	Gray matter bloodâ€brain barrier water exchange dynamics are reduced in progressive multiple sclerosis. Journal of Neuroimaging, 2021, 31, 1111-1118.	2.0	5
7	Intensity warping for multisite MRI harmonization. NeuroImage, 2020, 223, 117242.	4.2	34
8	Imaging Mechanisms of Disease Progression in Multiple Sclerosis: Beyond Brain Atrophy. Journal of Neuroimaging, 2020, 30, 251-266.	2.0	24
9	Distinguishing Extravascular from Intravascular Ferumoxytol Pools within the Brain: Proof of Concept in Patients with Treated Glioblastoma. American Journal of Neuroradiology, 2020, 41, 1193-1200.	2.4	8
10	Observation of Reduced Homeostatic Metabolic Activity and/or Coupling in White Matter Aging. Journal of Neuroimaging, 2020, 30, 658-665.	2.0	7
11	Modeling disease trajectory in Duchenne muscular dystrophy. Neurology, 2020, 94, e1622-e1633.	1.1	49
12	Multisite reliability and repeatability of an advanced brain MRI protocol. Journal of Magnetic Resonance Imaging, 2019, 50, 878-888.	3.4	27
13	Combined iron oxide nanoparticle ferumoxytol and gadolinium contrast enhanced MRI define glioblastoma pseudoprogression. Neuro-Oncology, 2019, 21, 517-526.	1.2	28
14	An Automated Statistical Technique for Counting Distinct Multiple Sclerosis Lesions. American Journal of Neuroradiology, 2018, 39, 626-633.	2.4	24
15	Baseline NAWM structural integrity and CBF predict periventricular WMH expansion over time. Neurology, 2018, 90, e2119-e2126.	1.1	69
16	Current and potential imaging applications of ferumoxytol for magnetic resonance imaging. Kidney International, 2017, 92, 47-66.	5.2	230
17	Pseudoâ€extravasation rate constant of dynamic susceptibility contrastâ€MRI determined from pharmacokinetic first principles. NMR in Biomedicine, 2017, 30, e3797.	2.8	0
18	Volumetric Analysis from a Harmonized Multisite Brain MRI Study of a Single Subject with Multiple Sclerosis. American Journal of Neuroradiology, 2017, 38, 1501-1509.	2.4	95

WILLIAM D ROONEY

#	Article	IF	CITATIONS
19	Comparison of cerebral blood flow and structural penumbras in relation to white matter hyperintensities: A multi-modal magnetic resonance imaging study. Journal of Cerebral Blood Flow and Metabolism, 2016, 36, 1528-1536.	4.3	62
20	Immunopathology of Japanese macaque encephalomyelitis is similar to multiple sclerosis. Journal of Neuroimmunology, 2016, 291, 1-10.	2.3	15
21	Mapping human brain capillary water lifetime: highâ€resolution metabolic neuroimaging. NMR in Biomedicine, 2015, 28, 607-623.	2.8	58
22	Longitudinal relaxographic imaging of white matter hyperintensities in the elderly. Fluids and Barriers of the CNS, 2014, 11, 24.	5.0	11
23	Intratumor mapping of intracellular water lifetime: metabolic images of breast cancer?. NMR in Biomedicine, 2014, 27, 760-773.	2.8	75
24	Pseudoprogression of Glioblastoma after Chemo- and Radiation Therapy: Diagnosis by Using Dynamic Susceptibility-weighted Contrast-enhanced Perfusion MR Imaging with Ferumoxytol versus Gadoteridol and Correlation with Survival. Radiology, 2013, 266, 842-852.	7.3	145
25	High-Resolution Steady-State Cerebral Blood Volume Maps in Patients with Central Nervous System Neoplasms Using Ferumoxytol, a Superparamagnetic Iron Oxide Nanoparticle. Journal of Cerebral Blood Flow and Metabolism, 2013, 33, 780-786.	4.3	94
26	Signal-to-noise ratio, contrast-to-noise ratio and pharmacokinetic modeling considerations in dynamic contrast-enhanced magnetic resonance imaging. Magnetic Resonance Imaging, 2012, 30, 1313-1322.	1.8	44
27	Cell membrane water exchange effects in prostate DCE-MRI. Journal of Magnetic Resonance, 2012, 218, 77-85.	2.1	30
28	Japanese macaque encephalomyelitis: A spontaneous multiple sclerosis–like disease in a nonhuman primate. Annals of Neurology, 2011, 70, 362-373.	5.3	46
29	Dynamic NMR effects in breast cancer dynamic-contrast-enhanced MRI. Proceedings of the National Academy of Sciences of the United States of America, 2008, 105, 17937-17942.	7.1	69
30	The magnetic resonance shutter speed discriminates vascular properties of malignant and benign breast tumors in vivo. Proceedings of the National Academy of Sciences of the United States of America, 2008, 105, 17943-17948.	7.1	85
31	Magnetic field and tissue dependencies of human brain longitudinal1H2O relaxation in vivo. Magnetic Resonance in Medicine, 2007, 57, 308-318.	3.0	546
32	Evidence for shutter-speed variation in CR bolus-tracking studies of human pathology. NMR in Biomedicine, 2005, 18, 173-185.	2.8	85
33	Shutter-speed analysis of contrast reagent bolus-tracking data: Preliminary observations in benign and malignant breast disease. Magnetic Resonance in Medicine, 2005, 53, 724-729.	3.0	67
34	A unified magnetic resonance imaging pharmacokinetic theory: Intravascular and extracellular contrast reagents. Magnetic Resonance in Medicine, 2005, 54, 1351-1359.	3.0	141
35	Recent advances in the neuroimaging of multiple sclerosis. Current Neurology and Neuroscience Reports, 2005, 5, 217-224.	4.2	6
36	Variation of the relaxographic ?shutter-speed? for transcytolemmal water exchange affects the CR bolus-tracking curve shape. Magnetic Resonance in Medicine, 2003, 50, 1151-1169.	3.0	171

WILLIAM D ROONEY

#	Article	IF	CITATIONS
37	The effects of equilibrium transcytolemmal water exchange on the determination of contrast reagent concentration in vivo. Magnetic Resonance in Medicine, 2002, 47, 422-424.	3.0	11
38	Reanalysis of multislice1H MRSI in amyotrophic lateral sclerosis. Magnetic Resonance in Medicine, 2001, 45, 513-516.	3.0	47
39	Determination of the MRI contrast agent concentration time course in vivo following bolus injection: Effect of equilibrium transcytolemmal water exchange. Magnetic Resonance in Medicine, 2000, 44, 563-574.	3.0	199
40	Resting brain metabolic activity in a 4 Tesla magnetic field. Magnetic Resonance in Medicine, 2000, 44, 701-705.	3.0	8
41	4.0 T Water Proton T1 Relaxation Times in Normal Human Brain and During Acute Ethanol Intoxication. Alcoholism: Clinical and Experimental Research, 2000, 24, 830-836.	2.4	14
42	Intimate combination of low- and high-resolution image data: I. real-space PET and1H2O MRI, PETAMRI. Magnetic Resonance in Medicine, 1999, 42, 345-360.	3.0	15